

Original Article

Open Access



# ZNF148/PFKP/PD-L1 axis promotes non-small cell lung cancer proliferation, migration and glycolysis

Jialiang Zhu<sup>1</sup>, Yufan Chen<sup>2</sup>, Longyu Jin<sup>1</sup>, Wei Feng<sup>1</sup>, Huaidong Hu<sup>1</sup>, Wenbo Xue<sup>1</sup>, Zhigang Zhou<sup>3</sup>, Guangyu Luo<sup>2</sup>

<sup>1</sup>Department of Cardiothoracic Surgery, The Third Xiangya Hospital of Central South University, Changsha 410013, Hunan, China.

<sup>2</sup>State Key Laboratory of Oncology in South China, Guangdong Provincial Clinical Research Center for Cancer, Sun Yat-sen University Cancer Center, Guangzhou 510060, Guangdong, China.

<sup>3</sup>Department of Oncology, Changde Hospital, Xiangya School of Medicine, Central South University, Changde 415003, Hunan, China.

**Correspondence to:** Dr. Zhigang Zhou, Department of Oncology, Changde Hospital, Xiangya School of Medicine, Central South University, No. 818 Renmin Road, Wuling District, Changde 415003, Hunan, China. E-mail: nhzhouzhigang@sina.com; Dr. Guangyu Luo, State Key Laboratory of Oncology in South China, Guangdong Provincial Clinical Research Center for Cancer, Sun Yat-sen University Cancer Center, 651 East Dongfeng Road, Yuexiu District, Guangzhou 510060, Guangdong, China. E-mail: luogy@sysucc.org.cn

**How to cite this article:** Zhu J, Chen Y, Jin L, Feng W, Hu H, Xue W, Zhou Z, Luo G. ZNF148/PFKP/PD-L1 axis promotes non-small cell lung cancer proliferation, migration and glycolysis. *J Cancer Metastasis Treat* 2023;9:42. <https://dx.doi.org/10.20517/2394-4722.2023.111>

**Received:** 20 Sep 2023 **First Decision:** 15 Nov 2023 **Revised:** 1 Dec 2023 **Accepted:** 20 Dec 2023 **Published:** 29 Dec 2023

**Academic Editor:** Ciro Isidoro **Copy Editor:** Fangyuan Liu **Production Editor:** Fangyuan Liu

## Abstract

**Aim:** Cancer-related deaths are primarily caused by lung cancer around the world. The prognosis and burden of lung cancer must be improved by identifying novel biomarkers for diagnosis and treatment. In non-small cell lung cancer (NSCLC), the platelet isoform of phosphofructokinase 1 (PFKP) has been identified as a tumor-promoting oncogene. The current study examined the specific role that PFKP plays in NSCLC tumorigenesis, as well as the underlying mechanism.

**Methods:** A lung cancer dataset was obtained from the TCGA in order to examine the expression of PFKP. Using the Kaplan-Meier Plotter website, we calculated the overall survival (OS) along with the recurrence-free survivals (RFS) curves with high and low levels of PFKP in lung cancer. The mechanism by which zinc finger protein 148 (ZNF148) regulated PFKP/PD-L1 levels in NSCLC was investigated through chromatin immunoprecipitation (ChIP), qRT-PCR, and western blotting. In order to uncover ZNF148's function in NSCLC, subsequent functional studies



© The Author(s) 2023. **Open Access** This article is licensed under a Creative Commons Attribution 4.0 International License (<https://creativecommons.org/licenses/by/4.0/>), which permits unrestricted use, sharing, adaptation, distribution and reproduction in any medium or format, for any purpose, even commercially, as long as you give appropriate credit to the original author(s) and the source, provide a link to the Creative Commons license, and indicate if changes were made.



included CCK-8, colony formation, and Transwell, along with glycolysis assays. Student's T-test was conducted for data analysis with GraphPad Prism 9.0.

**Results:** The expression of PFKP in NSCLC was increased, and it was linked to worse outcomes. This increased expression of PFKP in NSCLC was induced by ZNF148. Silencing ZNF148 remarkably dampened NSCLC cell proliferation, invasion, and glycolysis capacities. According to a mechanistic study, ZNF148 regulates the PFKP/PD-L1 axis, which promotes NSCLC tumorigenesis.

**Conclusion:** It has been established that ZNF148-induced PFKP is key to the proliferation, invasion, and glycolysis abilities of NSCLC cells by regulating PD-L1 expression. Therefore, the ZNF148/PFKP/PD-L1 axis could be a potential biological signature and target for NSCLC diagnosis and treatment.

**Keywords:** ZNF148, PFKP, PD-L1, NSCLC, proliferation

## INTRODUCTION

With improvements in early detection and precision medicine in recent years, such as immune checkpoint inhibition, lung cancer prognoses have improved in some cases<sup>[1]</sup>. Cancer-related deaths are primarily caused by lung cancer around the world, which poses a substantial burden on healthcare systems<sup>[2]</sup>. To reduce the burden of lung cancer, we must identify novel biomarkers for lung cancer patients to receive better diagnosis, treatment, and prognosis.

Phosphofructokinase 1 (PFKP) is an enzyme isoform that serves as a crucial mediator of glycolysis and cell metabolism. PFKP also plays a role in cancer progression<sup>[3]</sup>. PFKP is aberrantly upregulated in various cancers and promotes cancer growth and metastasis<sup>[4]</sup>. Specifically, in lung cancer, a high expression of PFKP correlates with a poor survival rate<sup>[5]</sup>. PFKP promotes lung cancer progression partly by regulating cell glycolysis and proliferation<sup>[6]</sup>. According to these findings, PFKP could be an interesting target for lung cancer treatment<sup>[7]</sup>. However, PFKP plays an unknown role in the tumorigenesis of NSCLC.

Zinc finger protein 148 (ZNF148) participates in tumor proliferation, invasion, and metastasis<sup>[8]</sup>. ZNF148 represses the activation of p53. ZNF148 deficiency leads to a reduction in cell proliferation<sup>[9]</sup>. In intestinal adenoma models, targeting ZNF148 markedly decreases tumor metastasis and improves survival by activating p53<sup>[10]</sup>. These results reveal that targeting ZNF148 might be useful for cancer patients. So far, neither the functions nor the mechanisms of ZNF148 in NSCLC progression have been identified.

Here, we explored the functions and regulatory mechanism of ZNF148-induced PFKP/PD-L1 in NSCLC. The PFKP was increased in NSCLC and correlated with poor outcomes. A ChIP assay confirmed that ZNF148 could directly bind to PFKP promoter and that high expression of PFKP in NSCLC was partly induced by ZNF148. Moreover, ZNF148 was markedly increased in cell lines along with tissues of NSCLC. Silencing ZNF148 significantly dampened NSCLC cell proliferation, invasion, and glycolysis capacities. A mechanistic experiment claimed that ZNF148 induced NSCLC tumorigenesis partially by modulating the PFKP/PD-L1 axis. Our study demonstrated the function of the ZNF148/PFKP/PD-L1 signaling in the NSCLC tumorigenesis process, which could provide promising targets for NSCLC patients.

## METHODS

### Data collection and analysis

The TCGA lung cancer cohort, which included 110 normal samples and 1,016 tumor samples, was obtained from the UCSC Xena project. Using the Kaplan-Meier Plotter website (<http://kmplot.com/analysis/index.php?>

[p=service&cancer=lung](#)), we calculated the overall survival (OS) along with recurrence-free survivals (RFS) curves with high and low levels of PFKP in lung cancer. All potential cutoff values within the lower and upper quartiles were computed using an automated selection process to identify the optimal cutoff value. The best-performing threshold determined through this process was subsequently adopted as the final cutoff value. Determined by auto select best cutoff that all possible cutoff values between the lower and upper quartiles are computed, and the best performing threshold is used as a cutoff.

The transcriptional regulatory region sequences of PFKP were acquired from the Ensembl database (<https://www.ensembl.org>). The subsequent search for potential transcription factors and binding sites was conducted with the JASPAR open-access database (<https://jaspar.genereg.net>).

### Cell culture

A human normal lung cell (Beas2b) along with NSCLC cells (A549, NCI-H358, PC9, NCI-H1975, HCC827 and H1299) were purchased from the ATCC (<https://www.atcc.org>, USA). A 37 °C incubator with 5% CO<sub>2</sub> cultivated cells in DMEM (Corning Life Sciences, USA). Authentication was conducted via short tandem repeat DNA profiling.

### Tissue specimens

During surgery at Central South University's Third Xiangya Hospital, 40 paired NSCLC samples (Tumor) along with adjacent normal tissues (Normal) were obtained. TRIzol (Invitrogen, USA) was used to preserve fresh tissues for qRT-PCR assays. Ethical approval was obtained from the Central South University Medical Ethics Committee, and the Declaration of Helsinki in 1964 was followed. Involved patients provided written informed consent. In accordance with the Helsinki Declaration, the procedure was performed.

### Quantitative real-time PCR (qRT-PCR)

A total RNA extract was obtained from NSCLC cells along with tissues using TRIzol (Invitrogen). SYBR® Premix Ex Taq™ (Takara, China) and Roche LightCycler® 480 II instrument were used. The following primer sequences were purchased from Invitrogen: PFKP forward, TCGGTCTCTCCAAGTTTGTGC, reverse, TTCCGTTGTCCACCAATCTGA; ZNF148 forward, TGATGATGCCATGCAGTTTT, reverse, TCCCTGCTGTTGTTACTTGCT. The mRNA levels were determined by the  $2^{-\Delta\Delta CT}$  formula.

### SiRNA transfection

si-ZNF148#1 (5'-AAGCATACTTTGAACTTTGC-3'), si-ZNF148#2 (5'-AATTCATTCCCTGATCGAAAGC-3'), si-ZNF148#3 (5'-AAGATCGAAGTATGCCTCACCTT-3') or si-NC were used to transfect A549, PC9, and H1299 cells with Lipofectamine 3000 (Invitrogen) in 6-well plates. Cells were harvested and used in subsequent experiments after transfection.

### Chromatin immunoprecipitation (ChIP)

A549, PC9, and H1299 cell lines were treated with 1% formaldehyde and glycine, as previously described<sup>[11]</sup>. Then, the cell lysates were sonicated, and the chromatin fraction was treated with either ZNF148 antibody (#sc-137171, Santa Cruz, USA) or IgG. Chromatin-bound beads were washed and eluted before protein digestion and DNA purification. Finally, the precipitated chromatin fragments were subjected to PCR.

### CCK-8 assay

A549, PC9, and H1299 cells were cultured ( $3 \times 10^3$  cells per well) in 96-well plates and then transfected with si-ZNF148. CCK-8 reagent (APEX-BIO, USA) was applied the next day for 2 h at 37 °C. An analysis of cell viability was conducted after measuring the absorbance at 490 nm.

### Colony formation assay

A549, PC9, and H1299 cells were cultured ( $1 \times 10^3$  cells per well) in 6-well plates and then transfected with si-ZNF148. Colonies were fixed in 4% paraformaldehyde after 2 weeks of culturing, and stained in 0.5% crystal violet. Finally, the colony numbers were calculated.

### Glycolytic metabolism assays

A Glucose Test Kit (Biovision, USA) was used to detect glucose consumption. A549, PC9, and H1299 cell lines treated with si-ZNF148 and cell culture medium were used to determine the glucose concentration reduction in the control cells ( $10^6$  cells/well). Lactate production was also determined using Lactate analyzers<sup>[12]</sup>. Si-ZNF148 or a control treatment was used to detect 2-NBDG uptake by a 2-NBDG Glucose Uptake Assay Kit (Abcam). Measurement of fluorescence was carried out with a microplate reader (Ex/Em = 485/535 nm).

### Immunofluorescence

A549, PC9, and H1299 cell lines were treated with si-ZNF148 or control. A PBS wash was followed by the fixation of the cells in methanol, followed by the blocking of the cells in 1% bovine serum albumin. After that, the cells were treated with antibodies, including GLUT1 (1:100, #AF5462, Affinity) and GLUT4 (1:200, #BF1001, Affinity). The cells were washed the next day before incubation by DAPI and a secondary antibody (Yeasen, China). Fluorescence microscopy was used to examine the cells finally.

### Western blotting

RIPA lysis buffer and PMSF were used to isolate protein, which was separated by 10% SDS-PAGE. Following the transfer of proteins onto PVDF membranes, the membranes were blocked with 5% skim milk. After that, PVDF membranes were treated by antibodies including PFKP (1:1,000, #ab119796, Abcam, USA), PD-L1 (1:1,000, #ab205921, Abcam), and GAPDH (1:1,000, #AF7021, Affinity, USA). The next day, secondary antibodies (1:5,000, #S0001 or #S0002, Affinity) were used on PVDF membranes for an hour. As a final step, enhanced chemiluminescence reagents (Yeasen) were used to detect the proteins. Relative grayscale values were calculated by ImageJ.

### Statistical analysis

We used GraphPad Prism 9.0 to perform our statistical analysis. Student's t-test confirmed that  $P \leq 0.05$  indicated significant significance. All data were collected from three repeated experiments, and presented as mean  $\pm$  SD of three repeated experiments.

## RESULTS

### PFKP was increased and correlated with poor patient outcomes in lung cancer

To explore the expression of PFKP in lung cancer samples and normal lung samples, a lung cancer dataset was downloaded from the TCGA database. The expression of PFKP was increased in cancerous lung tissues (Figure 1A,  $P < 0.0001$ ). Therefore, we investigated the roles of PFKP on prognosis. Data downloaded from the Kaplan-Meier Plotter website revealed that upregulated PFKP expression in lung cancer correlated with shortened OS ( $P = 2.8E-5$ , Figure 1B) and RFS ( $P = 0.0042$ , Figure 1C). Taken together, upregulated PFKP expression correlated with poor patient outcomes in lung cancer.

### ZNF148 was overexpressed and could upregulate the expression of PFKP in lung cancer

PFKP overexpression was then investigated further. JASPAR in silico analysis was used to identify the transcription factors that have potential binding sites within the transcriptional regulatory region of PFKP. Among the candidates, ZNF148 was selected for further investigation due to the six potential binding sites within the promotor of PFKP of ZNF148 with a homology higher than 90% [Figure 2A]. Thus, we explored

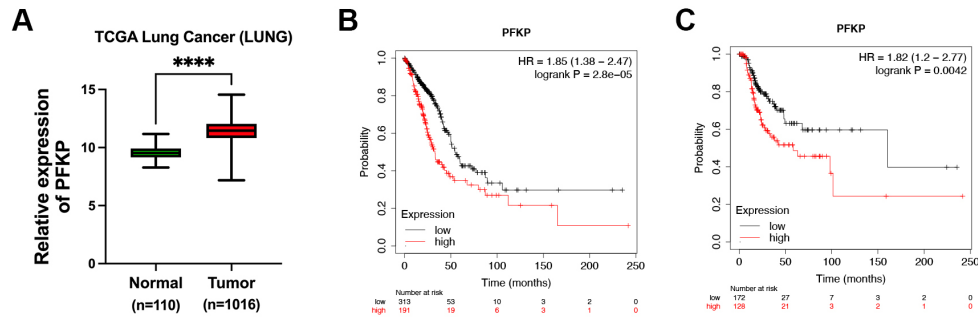


**Figure 1.** PFKP was increased and correlated with poor patient outcomes in lung cancer. (A) The levels of PFKP in lung cancer as well as normal lung samples. (B) Using the lung cancer dataset from the Kaplan-Meier Plotter website, the correlation between PFKP level and OS is shown. High or low PFKP expression was determined by auto select best cutoff with threshold 1,713. (C) The correlation between PFKP level and lung cancer patient RFS from the Kaplan-Meier Plotter website. High or low PFKP expression was determined by auto select best cutoff with threshold 1,557. \*\*\*\* $P < 0.0001$ .

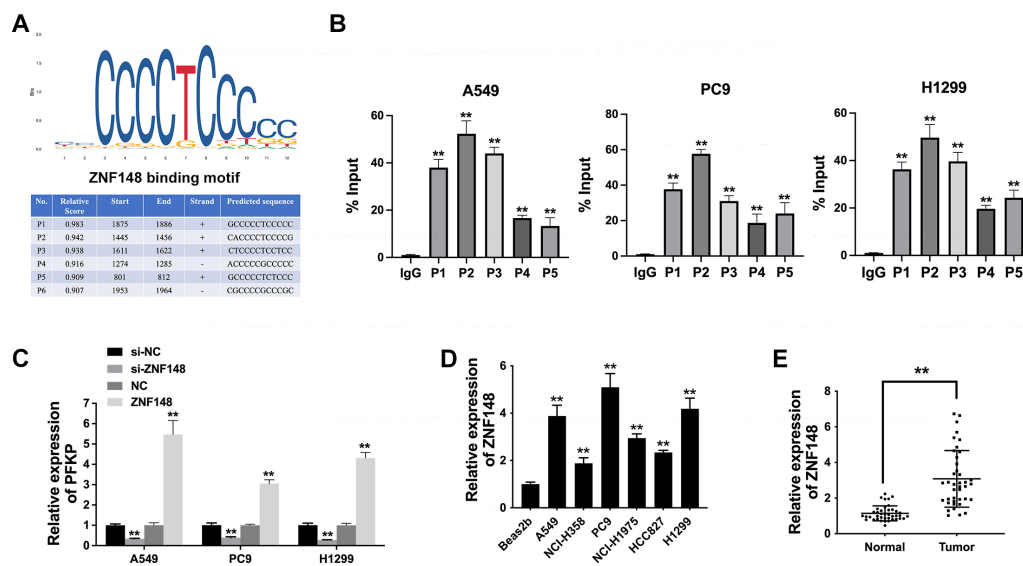


**Figure 2.** ZNF148 was overexpressed and could upregulate the expression of PFKP in lung cancer. (A) The potential ZNF148 binding sites within the promoter of the PFKP gene with a homology higher than 90% from JASPAR analysis are shown. (B) ChIP assay was performed with a ZNF148 antibody and analyzed with qPCR as a percent of the input. P1-P5 were the five ZNF148 potential binding sites within the promoter of PFKP. *P* values represent the comparison between IgG and P1-P5. (C) The expression of PFKP after transfection with si-ZNF148 or overexpression of ZNF148 and relative controls. *P* values represent the comparison between si-ZNF148 or si-NC and ZNF148 and NC. (D) ZNF148 levels were measured using qRT-PCR. *P* values represent the comparison between the human normal lung cell line Beas2b and each NSCLC cell line. (E) ZNF148 levels of 40 paired NSCLC samples (Tumor) along with adjacent normal samples (Normal). *P* values represent the comparison between tumor and normal tissues. \*\* $P < 0.01$ .

ZNF148’s direct interaction with PFKP promoter. ZNF148 is directly bound to the transcriptional regulatory region of PFKP [Figure 2B]. Subsequently, we investigated whether ZNF148 could regulate PFKP levels in NSCLC. ZNF148 overexpression could indeed increase PFKP levels. Moreover, ZNF148 inhibition reduced PFKP levels in NSCLC cells [Figure 2C]. We assessed the levels of ZNF148 and ZNF148, which were elevated in NSCLC cells, especially in A549, PC9, and H1299 [Figure 2D], which were used in the following experiments. Moreover, ZNF148 expression was verified in forty paired NSCLC and noncancerous tissue specimens. ZNF148 levels were significantly elevated in NSCLC tissues compared to noncancerous tissue specimens [Figure 2E].

### **NSCLC cell proliferation, invasion, and glycolysis were suppressed by ZNF148 inhibition**

To decrease ZNF148 expression, we used siRNAs in A549, PC9, along with H1299 cells. The ZNF148 level was strongly decreased after transfection with si-ZNF148#1 [Figure 3A]. The CCK-8 assay revealed that ZNF148 suppression inhibited NSCLC cell growth [Figure 3B]. Inhibition of ZNF148 inhibited NSCLC cell colony formation [Figure 3C and D]. Moreover, as demonstrated by Transwell, NSCLC cells were inhibited from invading by suppression of ZNF148 [Figure 3E and F]. Glycolytic metabolism plays a vital role in cancer progression<sup>[13]</sup>. We found that the expression levels of ZNF148 were elevated in NSCLC cell lines, especially in A549, PC9, and H1299. Therefore, we used these three cell lines in the following experiments to detect the effects of ZNF148 on glycolytic metabolism in NSCLC. NSCLC cells knocked down by ZNF148 consumed less glucose [Figure 3G], produced less lactate [Figure 3H], and reduced the ATP/ADP ratio [Figure 3I]. In addition, transfection of si-ZNF148 significantly reduced the uptake of 2-NBDG by NSCLC cells, indicating decreased glucose transport after ZNF148 knockdown [Figure 3J]. GLUT1 and GLUT4 are involved in glucose transport regulation and cell glucose uptake. Figure 3K shows that NSCLC cells transfected with si-ZNF148 showed decreased levels of GLUT1 and GLUT4, indicating decreased glucose availability to NSCLC cells after ZNF148 knockdown. Taken together, in NSCLC, downregulation of ZNF148 inhibited cell proliferation, invasion, and glycolysis.

### **ZNF148 modulated NSCLC tumorigenesis through the PFKP/PD-L1 axis**

The mechanism by which ZNF148 promotes NSCLC progression was explored. In glioblastoma, PFKP was reported to increase PD-L1 levels and enhance tumor immune evasion<sup>[14]</sup>. However, the impacts of PFKP on PD-L1 in NSCLC have not yet been explored. Thus, we investigated whether silencing ZNF148 suppressed PFKP-PD-L1 signaling in NSCLC. Western blotting showed that ZNF148 inhibition notably suppressed the levels of PFKP and PD-L1 in NSCLC [Figure 4A and B], indicating that ZNF148 could regulate the expression of PFKP, which could also modulate the expression of PD-L1. Altogether, these results revealed that ZNF148 promoted PFKP-PD-L1 pathway activation in NSCLC tumorigenesis.

## **DISCUSSION**

Despite recent advances in cancer screening and treatments, such as targeted therapy or immunotherapy, the outcome of NSCLC is still poor for most patients<sup>[15]</sup>. NSCLC is still a substantial global public health burden. Almost all NSCLC cases are diagnosed at advanced stages, resulting in worse survival. Therefore, the identification of new biomarkers is imperative for the diagnosis and treatment of lung cancer, as it is the key to improving patient outcomes<sup>[16-19]</sup>.

In hepatocellular carcinoma<sup>[20]</sup>, oral squamous cell carcinoma<sup>[21]</sup>, and lung cancer<sup>[22]</sup>, PFKP is a glycolysis enzyme involved in the tumor process. Cancer-associated fibroblasts (CAFs) play vital roles in tumor microenvironment. Tumor cells could interact with CAFs to promote the release of proinflammatory cytokines, consequently inducing glycolysis and thereby promoting cancer cell metastasis<sup>[23]</sup>. Suppressing CAF maturation and activation by induction of autophagy could inhibit their cross-talk with tumor cells to reverse the pro-tumor microenvironment<sup>[24]</sup>. It has been reported that the PFKP-AMPK interaction promotes the survival of glucose-starved NSCLC cells<sup>[25]</sup>. In NSCLC, hyperbaric oxygen therapy suppressed cell hyperproliferation and EMT by suppressing the HIF-1 $\alpha$ /PFKP axis<sup>[26]</sup>. Here, it has been demonstrated that PFKP is elevated and is associated with a worse prognosis of lung cancer [Figure 1], which indicates the possibility of using PFKP in NSCLC diagnostics and prognostics.

After investigating the regulatory mechanism of PFKP in NSCLC progression, we found that ZNF148 had potential binding sites within the promoter of PFKP, indicating that ZNF148 might interact with PFKP and regulate PFKP expression levels. Therefore, we confirm the direct binding between ZNF148 and PFKP

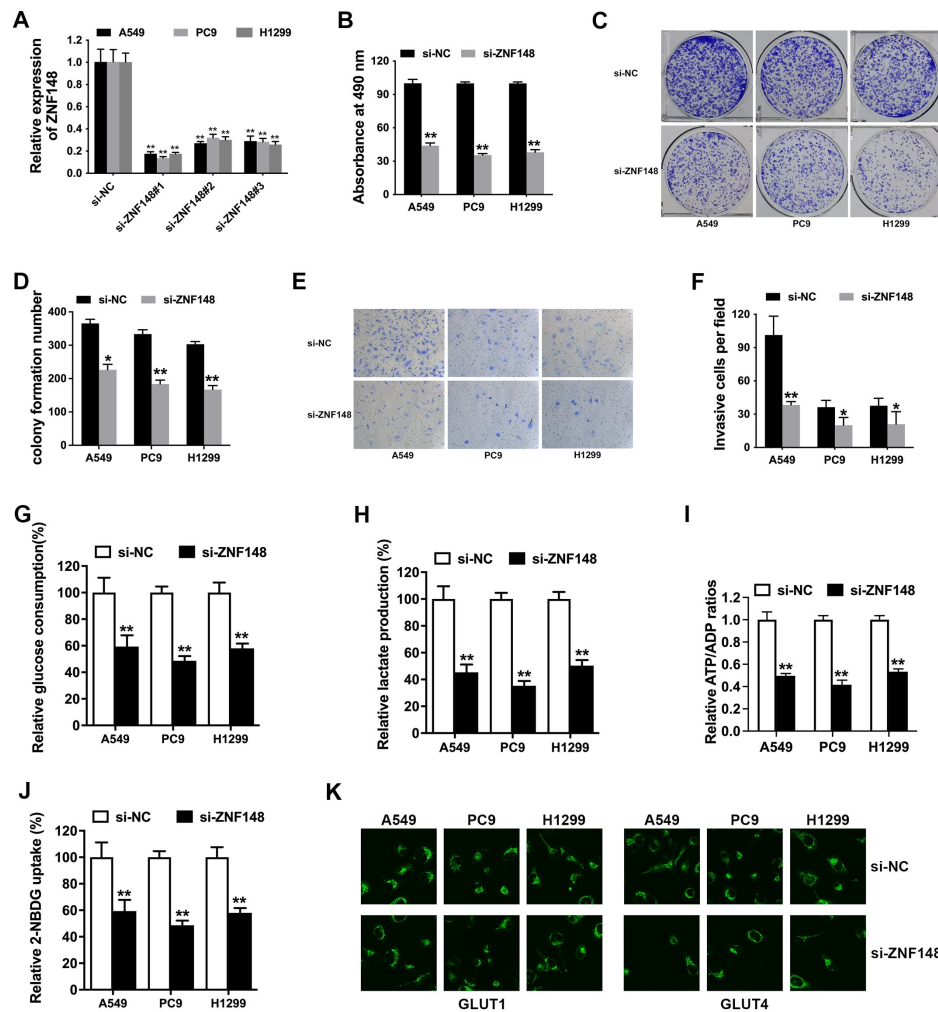


**Figure 3.** NSCLC cell proliferation, invasion, and glycolysis were suppressed by ZNF148 inhibition. (A) Transfections by si-ZNF148 or the control were performed on A549, PC9, and H1299 cells. *P* values represent the comparison between si-ZNF148 and si-NC in each cell line. (B) Cells were transfected with si-ZNF148 or the corresponding control and then cell growth was explored by CCK-8. *P* values represent the comparison between si-ZNF148 and si-NC in each cell line. (C) Cell growth was confirmed by colony formation analysis after transfection with si-ZNF148 or the corresponding control. (D) Statistical graph of colonies. *P* values represent the comparison between si-ZNF148 and si-NC in each cell line. (E) Transwell assays of A549, PC9, and H1299 cells after transfection with si-ZNF148 or the corresponding control. (F) The number of infiltrated cells was counted. *P* values represent the comparison between si-ZNF148 and si-NC in each cell line. (G) Glucose consumption in A549, PC9, and H1299 cells was determined after transfection with si-ZNF148 or the corresponding control. *P* values represent the comparison between si-ZNF148 and si-NC in each cell line. (H) Lactate production in A549, PC9, and H1299 cells was determined after transfection with si-ZNF148 or the corresponding control. *P* values represent the comparison between si-ZNF148 and si-NC in each cell line. (I) A549, PC9, and H1299 cells were transfected with si-ZNF148 or the corresponding control and then ATP/ADP ratios determined. *P* values represent the comparison between si-ZNF148 and si-NC in each cell line. (J) Relative 2-NBDG uptake in A549, PC9, and H1299 cells was determined after transfection with si-ZNF148 or the corresponding control. *P* values represent the comparison between si-ZNF148 and si-NC in each cell line. (K) Following si-ZNF148 transfection or control, immunofluorescence was used to determine GLUT1 and GLUT4 levels in A549, PC9 along with H1299 cells. \**P* < 0.05, \*\**P* < 0.01.

[Figure 2B]. Moreover, the qRT-PCR analysis showed that ZNF148 could regulate PFKP expression levels [Figure 2C]. ZNF148 was at the same time upregulated in NSCLC cell lines and tissues [Figures 2D and E], indicating that the overexpression of PFKP could be partly due to the elevated ZNF148 levels in NSCLC.

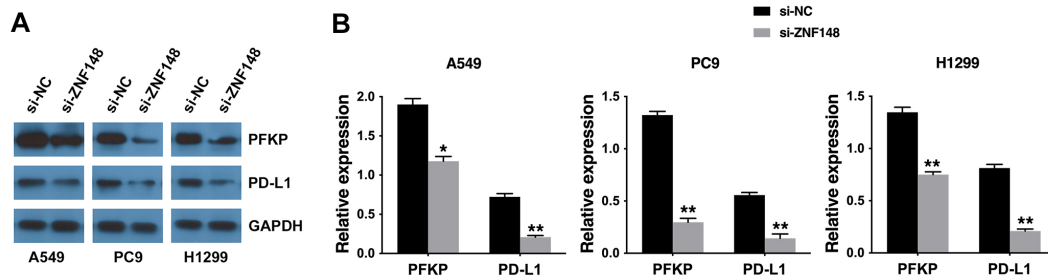


**Figure 4.** ZNF148 modulated NSCLC tumorigenesis through the PFKP/PD-L1 axis. (A) Western blotting of A549, PC9, and H1299 cells after transfection with si-ZNF148, and PFKP, PD-L1, and GAPDH expressions were detected. (B) The relative PFKP and PD-L1 levels determined with western blotting were quantified by ImageJ. *P* values represent the comparison between si-ZNF148 and si-NC in all cell lines. \**P* < 0.05, \*\**P* < 0.01.

ZNF148 is involved in multiple tumor processes. In esophageal cancer, it has been shown that ZNF148 is increased and correlated with a worse prognosis<sup>[27]</sup>. In gastrointestinal stromal tumors, ZNF148 promotes cell growth and invasion, and the ZNF148-S306 phosphorylation level is positively correlated with poor outcomes<sup>[28]</sup>. ZNF148 upregulation is also associated with distal metastasis in clear cell renal cell carcinoma<sup>[29]</sup>. However, the functions and mechanisms of ZNF148 in NSCLC progression are unclear. Here, we found that inhibition of ZNF148 could suppress NSCLC cell proliferation, invasion, and glycolysis [Figure 3], indicating that ZNF148 is vital in NSCLC progression, which could be a therapeutic target for NSCLC.

The final step was to investigate the mechanism of ZNF148 and PFKP in NSCLC progression. PFKP was reported to be involved in tumor immune evasion. In a previous study on T-cell malignancy, nuclear PFKP increased CXCR4 to induce T-ALL cell invasion and was correlated with poorer survival<sup>[30]</sup>. PD-L1 has crucial functions in cancer immune evasion<sup>[31]</sup>. PFKP can induce PD-L1 to enhance cancer immune evasion in glioblastoma<sup>[14]</sup>. In lung adenocarcinoma, PFKP has also been reported to be involved in tumor microenvironment immune cell infiltration<sup>[32]</sup>. However, the mechanisms by which PFKP regulates PD-L1 expression in NSCLC have not yet been fully explored. Here, we found that PFKP and PD-L1 expression in NSCLC was reduced by ZNF148 silencing [Figure 4]. Overall, these results suggest that ZNF148 contributes to NSCLC tumorigenesis partly via the PFKP-PD-L1 pathway.

## DECLARATIONS

### Authors' contributions

Conception and design of the study: Zhou Z, Luo G

Data acquisition: Zhu J, Chen Y, Jin L

Data analysis and interpretation: Feng W, Hu H, Xue W

The work drafting: Zhu J

The work substantively revising: Zhou Z, Luo G

### Availability of data and materials

All data and materials used in this study are available from the corresponding author upon reasonable request.

### Financial support and sponsorship

The Natural Science Foundation of Hunan Province (Nos. 2021JJ40919) funded this study.

### Conflicts of interest

All authors declare that there are no conflicts of interest.

### Ethical approval and consent to participate

The Medical Ethics Committee of Central South University approved the study involving human participants, and the Declaration of Helsinki in 1964 was followed. Informed consent was provided by all participants.

### Consent for publication

Informed consent for publication was provided by all participants.

### Copyright

© The Author(s) 2023.

### REFERENCES

1. Dumonceau JM, Tringali A, Papanikolaou IS, et al. Endoscopic biliary stenting: indications, choice of stents, and results: European Society of Gastrointestinal Endoscopy (ESGE) clinical guideline - updated October 2017. *Endoscopy* 2018;50:910-30. DOI
2. Sung H, Ferlay J, Siegel RL, et al. Global cancer statistics 2020: GLOBOCAN estimates of incidence and mortality worldwide for 36 cancers in 185 countries. *CA Cancer J Clin* 2021;71:209-49. DOI
3. Lang L, Chemmalakuzhy R, Shay C, Teng Y. PFKP signaling at a glance: an emerging mediator of cancer cell metabolism. In: Guest PC, editor. *Reviews on biomarker studies of metabolic and metabolism-related disorders*. Cham: Springer International Publishing; 2019. pp. 243-58. DOI
4. Lee JH, Liu R, Li J, et al. Stabilization of phosphofructokinase 1 platelet isoform by AKT promotes tumorigenesis. *Nat Commun* 2017;8:949. DOI PubMed PMC
5. Lee SY, Jin CC, Choi JE, et al. Genetic polymorphisms in glycolytic pathway are associated with the prognosis of patients with early stage non-small cell lung cancer. *Sci Rep* 2016;6:35603. DOI
6. Shen J, Jin Z, Lv H, et al. PFKP is highly expressed in lung cancer and regulates glucose metabolism. *Cell Oncol* 2020;43:617-29. DOI
7. Wang F, Li L, Zhang Z. Platelet isoform of phosphofructokinase promotes aerobic glycolysis and the progression of non-small cell lung cancer. *Mol Med Rep* 2021;23:74. DOI PubMed PMC
8. Zhang CZ, Chen GG, Lai PB. Transcription factor ZBP-89 in cancer growth and apoptosis. *Biochim Biophys Acta* 2010;1806:36-41. DOI PubMed
9. Zou ZV, Gul N, Lindberg M, et al. Genomic profiling of the transcription factor Zfp148 and its impact on the p53 pathway. *Sci Rep* 2020;10:14156. DOI PubMed PMC
10. Nilton A, Sayin VI, Zou ZV, et al. Targeting Zfp148 activates p53 and reduces tumor initiation in the gut. *Oncotarget* 2016;7:56183-92. DOI PubMed PMC
11. Essien BE, Sundaresan S, Ocadiz-Ruiz R, et al. Transcription factor ZBP-89 drives a feedforward loop of  $\beta$ -catenin expression in colorectal cancer. *Cancer Res* 2016;76:6877-87. DOI PubMed PMC
12. Liu L, Wang Y, Bai R, Yang K, Tian Z. MiR-186 inhibited aerobic glycolysis in gastric cancer via HIF-1 $\alpha$  regulation. *Oncogenesis* 2017;6:e318. PubMed PMC
13. Zhou Z, Qin J, Song C, et al. circROBO1 promotes prostate cancer growth and enzalutamide resistance via accelerating glycolysis. *J Cancer* 2023;14:2574-84. DOI PubMed PMC
14. Wang S, Park SH, Lim JS, Park YY, Du L, Lee JH. Phosphofructokinase 1 platelet isoform induces PD-L1 expression to promote glioblastoma immune evasion. *Genes Genomics* 2022;44:1509-17. DOI PubMed
15. Miller M, Hanna N. Advances in systemic therapy for non-small cell lung cancer. *BMJ* 2021;375:n2363. DOI PubMed
16. Oliver AL. Lung Cancer: Epidemiology and screening. *Surg Clin North Am* 2022;102:335-44. DOI PubMed
17. Liu P, Wang Z, Ou X, et al. The FUS/circEZH2/KLF5/ feedback loop contributes to CXCR4-induced liver metastasis of breast cancer by enhancing epithelial-mesenchymal transition. *Mol Cancer* 2022;21:198. DOI PubMed PMC
18. Yu Z, Tang H, Chen S, et al. Exosomal LOC85009 inhibits docetaxel resistance in lung adenocarcinoma through regulating ATG5-induced autophagy. *Drug Resist Updat* 2022;67:100915. DOI
19. Zou Y, Ye F, Kong Y, et al. The single-cell landscape of intratumoral heterogeneity and the immunosuppressive microenvironment in liver and brain metastases of breast cancer. *Adv Sci* 2023;10:e2203699. DOI PubMed PMC
20. Sha X, Wang K, Wang F, Zhang C, Yang L, Zhu X. Silencing PFKP restrains the stemness of hepatocellular carcinoma cells. *Exp Cell Res* 2021;407:112789. DOI
21. Chen G, Liu H, Zhang Y, et al. Silencing PFKP inhibits starvation-induced autophagy, glycolysis, and epithelial mesenchymal transition in oral squamous cell carcinoma. *Exp Cell Res* 2018;370:46-57. DOI

22. Wang Y, Mei Q, Ai YQ, et al. Identification of lung cancer oncogenes based on the mRNA expression and single nucleotide polymorphism profile data. *Neoplasma* 2015;62:966-73. [DOI](#)
23. Vidoni C, Ferraresi A, Vallino L, et al. Glycolysis inhibition of autophagy drives malignancy in ovarian cancer: exacerbation by IL-6 and attenuation by resveratrol. *Int J Mol Sci* 2023;24:1723. [DOI](#) [PubMed](#) [PMC](#)
24. Savio M, Ferraresi A, Corpina C, et al. Resveratrol and its analogue 4,4'-dihydroxy-trans-stilbene inhibit lewis lung carcinoma growth in vivo through apoptosis, autophagy and modulation of the tumour microenvironment in a murine model. *Biomedicines* 2022;10:1784. [DOI](#) [PubMed](#) [PMC](#)
25. Chen J, Zou L, Lu G, et al. PFKP alleviates glucose starvation-induced metabolic stress in lung cancer cells via AMPK-ACC2 dependent fatty acid oxidation. *Cell Discov* 2022;8:52. [DOI](#) [PubMed](#) [PMC](#)
26. Zhang L, Ke J, Min S, et al. Hyperbaric oxygen therapy represses the warburg effect and epithelial-mesenchymal transition in hypoxic NSCLC cells via the HIF-1 $\alpha$ /PFKP axis. *Front Oncol* 2021;11:691762. [DOI](#) [PubMed](#) [PMC](#)
27. Yan SM, Wu HN, He F, et al. High expression of zinc-binding protein-89 predicts decreased survival in esophageal squamous cell cancer. *Ann Thorac Surg* 2014;97:1966-73. [DOI](#)
28. Gao X, Ma C, Sun X, et al. Upregulation of ZNF148 in SDHB-deficient gastrointestinal stromal tumor potentiates Forkhead box M1-mediated transcription and promotes tumor cell invasion. *Cancer Sci* 2020;111:1266-78. [DOI](#) [PubMed](#) [PMC](#)
29. Cai MY, Luo RZ, Li YH, et al. High-expression of ZBP-89 correlates with distal metastasis and poor prognosis of patients in clear cell renal cell carcinoma. *Biochem Biophys Res Commun* 2012;426:636-42. [DOI](#)
30. Gao X, Qin S, Wu Y, et al. Nuclear PFKP promotes CXCR4-dependent infiltration by T cell acute lymphoblastic leukemia. *J Clin Invest* 2021;131:e143119. [DOI](#) [PubMed](#) [PMC](#)
31. Huang X, Xie X, Wang H, et al. PDL1 And LDHA act as ceRNAs in triple negative breast cancer by regulating miR-34a. *J Exp Clin Cancer Res* 2017;36:129. [DOI](#) [PubMed](#) [PMC](#)
32. Dai Z, Liu T, Liu G, et al. Identification of clinical and tumor microenvironment characteristics of hypoxia-related risk signature in lung adenocarcinoma. *Front Mol Biosci* 2021;8:757421. [DOI](#) [PubMed](#) [PMC](#)